Jpn. J. Appl. Phys. Vol. 38 (1999) pp. 535–538
Part 1, No. 1B, January 1999

Optical and Resonant Tunnelling Spectroscopy of Self-Assembled Quantum Dot Systems

Antonio POLIMENI, Amalia PATANÈ, Andrew THORNTON, Thomas IHN, Laurence EAVES, Peter MAIN, Mohamed HENINI and Geoffrey HILL[1]

School of Physics and Astronomy, University of Nottingham, NG7 2RD Nottingham, United Kingdom
[1]*Department of Electronic and Electrical Engineering, University of Sheffield, Mappin Street, Sheffield S1 3JD, United Kingdom*

(Received June 1, 1998; accepted for publication October 22, 1998)

The electronic properties of self-assembled quantum dots have been studied by means of optical and tunnelling spectroscopy. The effect of confining barrier composition and design on the thermal behaviour of the dot optical properties is reported and exploited for the realisation of quantum dot based lasers. Tunnel current spectroscopy through a single discrete quantum dot state is used to investigate the electronic properties of an adjacent two-dimensional electron gas, including the Landau level density of states and many-body enhanced g-factor in the presence of a magnetic field.

KEYWORDS: self-assembled quantum dots, molecular beam epitaxy, photoluminescence, laser devices, resonant tunnelling diode, two-dimensional electron gas

1. Introduction

This paper is an overview of the recent work done by our group at Nottingham on the unique properties of self-assembled quantum dots (QD)[1)] as determined by optical and resonant tunnelling spectroscopy. The QDs are nominally composed of InAs or $In_xGa_{1-x}As$ embedded in GaAs and $Al_yGa_{1-y}As$ matrices and grown by molecular beam epitaxy. The paper is arranged as follows. In §2 we report on the effect of confining barrier design on the thermal behaviour of the dot photoluminescence (PL). On the basis of this study a QD-based laser has been fabricated and its properties studied as a function of temperature (§3). In §4 the electron resonant tunnelling at high magnetic fields (B) through the zero-dimensional state of a QD is described.

2. Influence of the Confining Potential on the Thermal Behaviour of the QD Luminescence

The study of QD optical properties by varying the lattice temperature, T, is of great interest for device applications such as QD lasers. In order to improve the thermal stability of the dot optical properties, we investigated the influence of the QD confining barrier design and composition on them. Two different structures are considered: the first one (a) consists of three InAs layers, 1.8-monolayer (ML)-thick, separated by 20 nm, each embedded in an $Al_yGa_{1-y}As$ matrix having Al content $y = 0.0$, 0.15 or 0.3. The growth temperature for this structure was $T_G = 520$°C. In the second structure (b) ($T_G = 500$°C) the dots are embedded in each of three $Al_{0.3}Ga_{0.7}As$/GaAs quantum wells (QW) with a width each of 10 nm, separated by barriers of 10 nm. A sketch of the conduction band profile is shown in Fig. 1. We do not expect the dot size and shape to change dramatically for QDs embedded in $Al_yGa_{1-y}As$ ($y \leq 0.3$) matrices. In fact scanning trasmission microscopy studies performed on InAs/AlAs QDs showed that the dot diameter, d, was slightly smaller ($d \sim 10$ nm) with respect to InAs/GaAs QDs ($d \sim 15$ nm). For photoluminescence (PL) measurements, the 514.5-nm line of an Ar^+ laser provided optical excitation. The luminescence was dispersed by a 3/4-m monochromator and detected by a cooled Ge diode detector.

Figure 2 shows the room temperature (RT) PL spectra of the different structures studied. A clear blue-shift of the QD luminescence can be observed in structure (a) with increasing y along with a broadening of the dot energy distribution, due to a possible alloy disorder induced by the (AlGa)As barrier. Structure (b) has similar a PL peak position and linewidth as structure (a) with $y = 0.0$ indicating that the outer QW (AlGa)As barrier does not much affect the energy position of the QD levels. In regard to the PL intensity, the samples in the $y = 0.3$ (AlGa)As matrix (both structures (a) and (b)) show the highest PL intensity at room temperature. This is a consequence of the reduced thermal escape of the carriers from the dots provided by the higher confining barrier. The wetting layer does not contribute significantly to the carrier escape as can be deduced from its small PL intensity compared to the QD emission (see Fig. 2). Figure 3 shows the PL integrated intensity as a function of temperature for the different structures considered. The dramatic effect of the barrier design can be clearly observed. A decrease of the PL integrated intensity of less than an order of magnitude was found for $y = 0.3$ (structure (a)) from $T = 10$ K up to RT, and of one order of magnitude for the dots embedded in the GaAs/$Al_{0.3}Ga_{0.7}As$ quantum well (structure (b)). The different slopes of the curves at the higher T are due to the different channels responsible for the luminescence quenching. A single activation energy cannot be determined from the data, indicating that a complex mechanism governs the thermal carrier escape from the dots.

3. Laser Devices Based on Self-Assembled QDs

In this part we describe the operation of a laser having QDs as active material. For the design we chose the structure (b) described above in order to exploit the good thermal behaviour and the narrower dot energy distribution (smaller PL linewidth) of this sample. For the laser-active material, the dots are formed by depositing a 1.1 nm-thick $In_{0.5}Ga_{0.5}As$ layer in the centre of each GaAs/$Al_{0.3}Ga_{0.7}As$ QW. (InGa)As dots were chosen as the active medium because they provide smaller threshold currents relative to InAs QDs embedded in the same structure. The cavity was clad by 1.5 μm of $Al_{0.6}Ga_{0.4}As$ (the latter layer is n-doped on the substrate side and p-doped on the top side). The QDs and the cavity were grown at 450°C and the (AlGa)As cladding layer at 600°C.

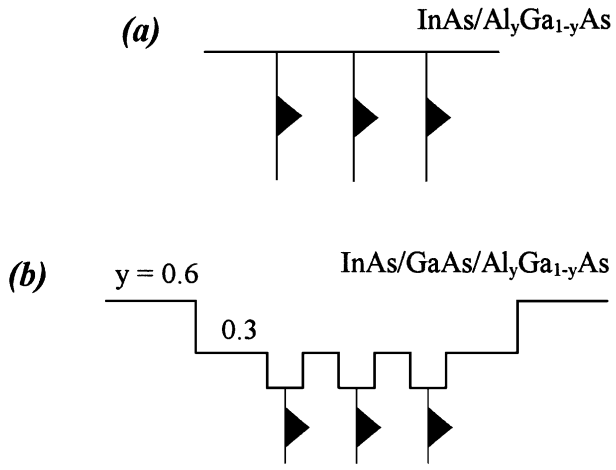

Fig. 1. Sketch of the different confining potentials considered.

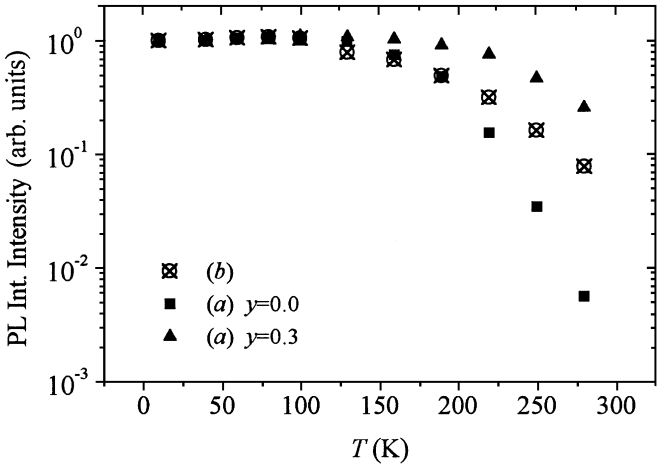

Fig. 3. Integrated PL intensity dependence on temperature for each of the different confining potentials considered ($P = 60\,\mathrm{W/cm^2}$, $\lambda_{exc} = 514.5\,\mathrm{nm}$).

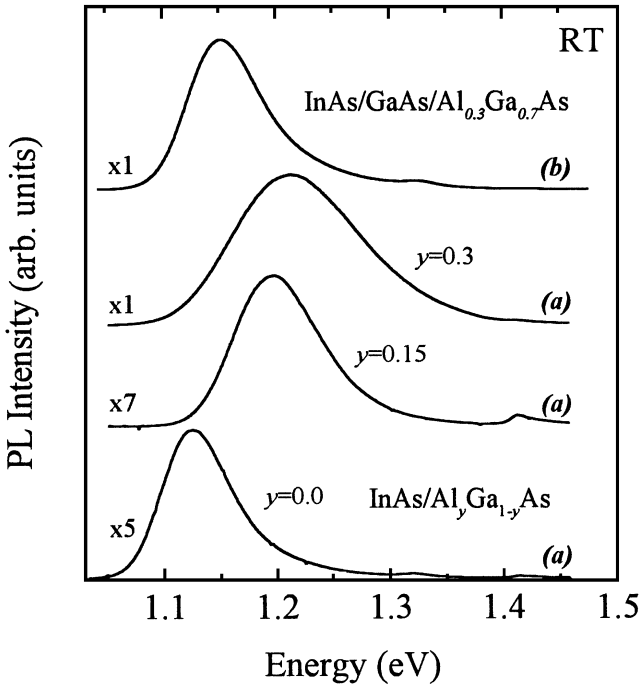

Fig. 2. Room temperature PL spectra for different InAs/GaAs/$Al_yGa_{1-y}As$ QD structures. The spectrum intensities are normalised to each other; the normalisation factor is shown for each spectrum (left side). Laser power density $P = 400\,\mathrm{W/cm^2}$ and excitation wavelength $\lambda_{exc} = 514.5\,\mathrm{nm}$.

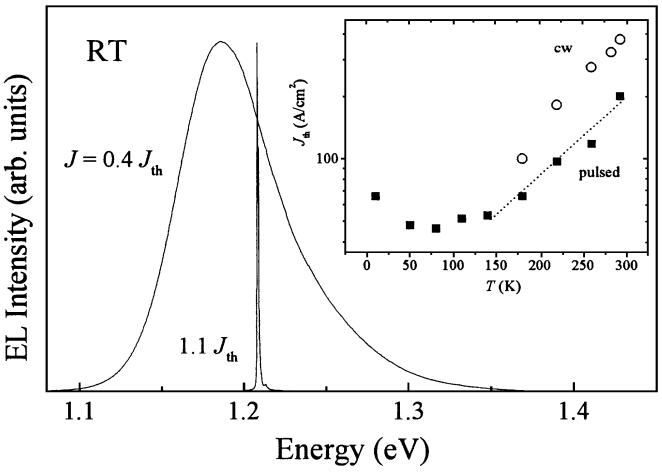

Fig. 4. Room temperature pulsed mode (0.2 μs pulse and 5% duty cycle) EL spectra for an $In_{0.5}Ga_{0.5}As/GaAs/Al_{0.3}Ga_{0.7}As$ QD laser below and above the threshold current J_{th} (=200 A/cm^2). The inset shows the dependence on temperature of the threshold current density in pulsed (filled squares) and cw (clear circles) mode. The dotted line indicates the best fit to the data using $J_{th} = J_0 \exp(T/T_0)$ with $T_0 = 110\,\mathrm{K}$.

The samples were grown on a (100) GaAs substrate. The devices studied are index-guided, in-plane lasers produced by standard etching and lithography. The cavity length is 2 mm, with a width of 15 μm. Laser characteristics were studied both under pulsed (0.2 μs pulse and 5% duty cycle) and continuous wave (cw) operation for T ranging from 10 K to room temperature.

Figure 4 shows the RT pulse mode EL spectra below and above the threshold current, J_{th}, of a laser having the structure described above. The value of J_{th} is 200 A/cm^2. This value compares with the best reported in literature.[2)] The T dependence of the pulse mode J_{th} is shown in Fig. 4, inset. The cw values of J_{th} are also reported for a higher temperature range. Note the presence of a minimum J_{th} for $T = 80\,\mathrm{K}$. This behaviour can be explained by considering that at low temperatures the carriers are frozen randomly into the energetic distribution determined by the dot size ensemble. As a consequence, a large fraction of carriers cannot take part in the lasing action which possibly involves only a small number of dots. By increasing the temperature, the detrapping of carriers from the dots results in a larger number of electrons and holes available for lasing; hence a smaller threshold current results with increasing T. This effect is then contrasted by the thermal increase of J_{th} and thus a minimum J_{th} is observed. The same behaviour has been reported in ref. 3. The increase of J_{th} with T can be described by $J_{th} = J_0 \exp(T/T_0)$. In our case we find a characteristic temperature, $T_0 = 110\,\mathrm{K}$ for T between 140 K and 290 K. At cryogenic temperatures ($80\,\mathrm{K} < T < 180\,\mathrm{K}$) T_0 becomes as large as 290 K.

Figure 5 shows the EL spectra above the threshold current at different temperatures. The laser luminescence spectra are characterised by a multi-mode emission, whose energy spac-

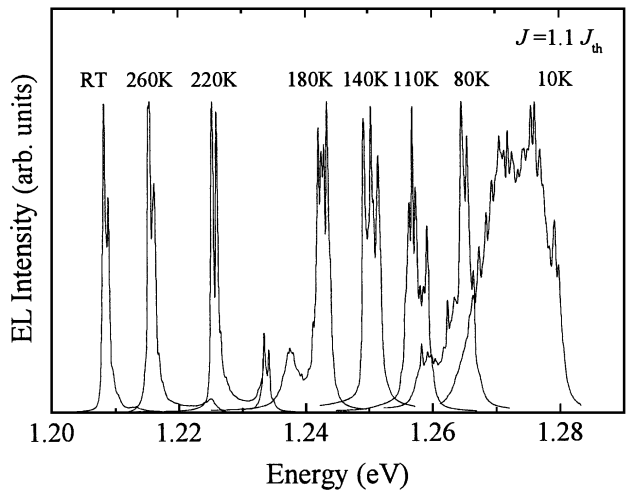

Fig. 5. Above threshold ($J = 1.1J_{\rm th}$) pulsed mode (0.2 μs pulse and 5% duty cycle) EL spectra at different temperatures for the laser structure shown in Fig. 4. Note the strong narrowing of the mode distribution with increasing T.

ing is not related to cavity length. The relative intensity of the modes strongly depends on the temperature and an interesting narrowing of their distribution can be observed with increasing T. The random size distribution of the dots can be invoked to explain the large linewidth of the laser spectrum at $T = 5\,\mathrm{K}$. Then a higher value of the temperature might allow an enhanced carrier drift towards the dots where the lasing action preferentially takes place. Finally, at room temperature this gives rise to a laser spectrum having a single mode. Further investigations are needed to better clarify this anomalous behaviour.

4. Electron Resonant Tunnelling through the Zero-Dimensional State of a QD

Recently we reported on an investigation of electron tunnelling through the discrete state of InAs quantum dots embedded in the AlAs barrier of a GaAs/AlAs/GaAs heterostructure.[4,5] At low temperatures ($T \leq 4\,\mathrm{K}$), sharp peaks are observed in the current-voltage characteristics $I(V)$, each peak corresponding to the tunnelling through a single quantum dot. The electrons tunnel from a two-dimensional electron gas (2DEG) which forms in an accumulation layer adjacent to the barrier when the device is biased. Investigations on similar a type of structure have also been carried out by Narihiro *et al.*[6] and Suzuki *et al.*[7]

In this section we demonstrate the use of a single InAs self-assembled quantum dot, to probe the local density of states (LDOS) of the 2DEG for all energies between the Fermi energy and the 2DEG subband edge. Note that conventional magneto-transport measurements of two-dimensional electron systems are sensitive only to effects at the Fermi energy, $\varepsilon_{\rm F}$. Full details of the device are given in ref. 4. In a current-voltage sweep ($I(V)$), we see distinct peaks due to electrons tunnelling from the 2DEG through single InAs QDs. As we increase the voltage across the device, the ground state of the QD is moved down relative to the Fermi level of the 2DEG. Tunnelling occurs as the ground state of the dot crosses the Fermi level of the 2DEG, and continues until the ground state is moved below the 2DEG subband edge. The tunnel current

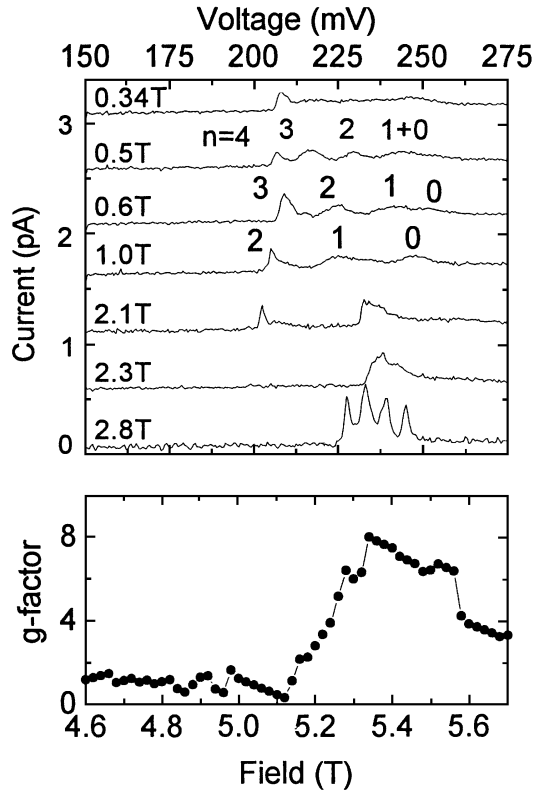

Fig. 6. Current-voltage sweeps in a constant magnetic field (top), and the g-factor against magnetic field, around filling factor 1 (bottom).

measured is a direct measure of the LDOS of the 2DEG, and in this way we are able to probe the LDOS of the 2DEG at all energies between $\varepsilon_{\rm F}$ and the subband edge. It should be noted that low voltage in $I(V)$ corresponds to a high energy in the 2DEG.

We have used this technique, with a magnetic field, B, applied parallel to the current, to probe the occupied Landau Levels (LL) in the 2DEG. Figure 6 (upper box) shows a typical series of $I(V)$ curves obtained at different fields at a temperature of 100 mK. A number of effects are observed. For $B > 0.42\,\mathrm{T}$, we resolve the $n = 4$, 3, and 2 LLs, but $n = 0$ and 1, which are well below $\varepsilon_{\rm F}$, are not resolved until higher values of $B > 0.6\,\mathrm{T}$ (see Fig. 6). This is interpreted tentatively in terms of a quasiparticle lifetime effect which broadens the width of Landau levels well below the Fermi energy. The magnetic field dependence of our measured resolved linewidths fits well with the Ando and Uemura theory,[8] shown as the solid curve in Fig. 7.

At higher fields close to the filling factor 1 ($\nu = 1$) around 5.2 T, we observe a spin splitting effect which directly reveals the many-body enhancement of the effective Landè g-factor, g^* of the 2DEG. In the vicinity of $\nu = 1$, the peak in $I(V)$ corresponding to the lowest energy, spin-polarised LL shifts to higher voltage, or *lower* energy, with increasing B. This can be interpreted as an increase in g^* of the 2DEG which is plotted in the lower box of Fig. 6. The increase is in qualitative agreement with that obtained by Dolgopolov *et al.*[9]

5. Conclusions

We have described a wide range of experiments in which the properties of self-assembled quantum dots are exploited.

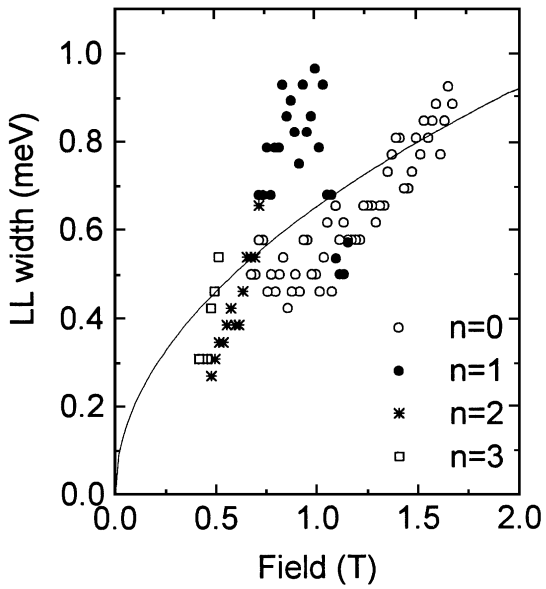

Fig. 7. Landau level widths versus magnetic field for the first four levels. The fitted curve demonstrates the $B^{1/2}$ dependence.

We studied the optical properties of the dots at different temperatures and found the optimal design for the confining barrier. The same design has been used for the realisation of a laser working up to room temperature. The zero-dimensional properties of the dots have also been successfully used in the investigation of the local density of states and the enhanced g-factor of a two-dimensional electron gas.

Acknowledgement

This work and Laurence Eaves are supported by the Engineering and Physical Sciences Research Council (EPSRC).

1) J.-Y. Marzin, J.-M. Gérard, A. Izraël, D. Barrier and G. Bastard: Phys. Rev. Lett. **64** (1994) 716.
2) N. N. Ledentsov, V. A. Shchukin, M. Grundmann, N. Kirstaedter, J. Böhrer, O. Schmidt, D. Bimberg, V. M. Ustinov, A. Yu. Egorov, A. E. Zhukov, P. S. Kop'ev, S. V. Zaitsev, N. Yu. Gordeev, Zh. I. Alferov, A. I. Borovkov, A. Kosogov, S. S. Ruminov, P. Werner, U. Gösele and J. Heydenreich: Phys. Rev. B **54** (1996) 8743.
3) A. E. Zhukov, V. M. Ustinov, A. Yu. Egorov, A. R. Kovsh, A. F. Tsatsulnikov, N. N. Ledentsov, S. V. Zaitsev, N. Yu. Gordeev, P. S. Kop'ev and Zh. I. Alferov: Jpn. J. Appl. Phys. **36** (1997) 4216.
4) I. E. Itskevich, T. Ihn, A. Thornton, M. Henini, T. J. Foster, P. J. Moriarty, A. Nogaret, P. H. Beton, L. Eaves and P. C. Main: Phys. Rev. B **54** (1996) 16401.
5) A. Thornton, T. Ihn, P. C. Main, L. Eaves, K. A. Benedict and M. Henini: Physica B **249–251** (1998) 689.
6) M. Narihiro, G. Yusa, Y. Nakamura, T. Noda and H. Sakaki: Appl. Phys. Lett. **70** (1997) 105.
7) T. Suzuki, K. Nomoto, K. Taira and I. Hase: *Ext. Abstr. Proc. Int. Conf. Solid State Devices and Materials* (Business Center for Academic Societies Japan, Tokyo, 1996) p. 691.
8) T. Ando and Y. Uemura: J. Phys. Soc. Jpn. **36** (1967) 959.
9) V. T. Dolgopolov, A. A. Shashkin, A. V. Aristov, D. Schmerek, W. Hansen, J. P. Kotthaus and M. Holland: Phys. Rev. Lett. **79** (1997) 729.